Charged Current Interactions at HERA

Kruse, A.

Publication date
1999

Citation for published version (APA):
Kruse, A. (1999). *Charged Current Interactions at HERA*.

Chapter 3

The *HERA* machine and the *ZEUS* detector

3.1 The *HERA* Particle Accelerator

The "Hadron-Elektron-Ring-Anlage" (*HERA*) was built from 1984 to 1992 at the "Deutsche Elektronen Synchrotron" (*DESY*) laboratory in Germany and is the world's largest Electron-Proton collider.

HERA consists of two storage rings, one for protons and one for electrons (or positrons). It is built below surface in a near-circular tunnel of 6.336 km circumference. It has four experimental underground halls, of which two are used by general purpose electron-proton collision experiments, *H1* [15] and *ZEUS* [16]. The other two are used by *HERMES* which uses the electron beam on a polarized gas target to study the origin of nucleon spin and *HERA-B* which studies CP violation in B-meson decays using the proton beam on an internal wire target. Both of these experiments use the beams parasitically.

In the proton ring super conducting magnets are used to store the protons which have an energy of 820 GeV. The electron ring has super conducting *R.F.* cavities to accelerate the electrons and during storage to compensate for the loss of energy due to synchrotron radiation. The electron beams have an energy of 27.52 GeV.

At the *H1* and *ZEUS* experimental halls a combination of dipole and quadrupole magnets is used to bring the two beams into head-on collision and to provide the final focus for the beams.

Figure 3.1 shows a schematic view of *HERA* and its pre-accelerators, table 3.1 lists the main design parameters for *HERA*.

3.1.1 Bunch Structure

Both the positron and proton beams are stored in a total of 220 *R.F.* buckets. This yields a bunch structure of the beam with a time between two successive e-p bunch collisions of 96 ns.

Not all of the 220 bunches are filled. This allows background studies to be performed. Events that occur when only a positron or only a proton bunch pass the detector can be used to evaluate the background from beam gas interactions. Whereas times when neither proton nor positron pass the detector allow investigation of the noise characteristics of the detector and of the backgrounds due to cosmic rays.

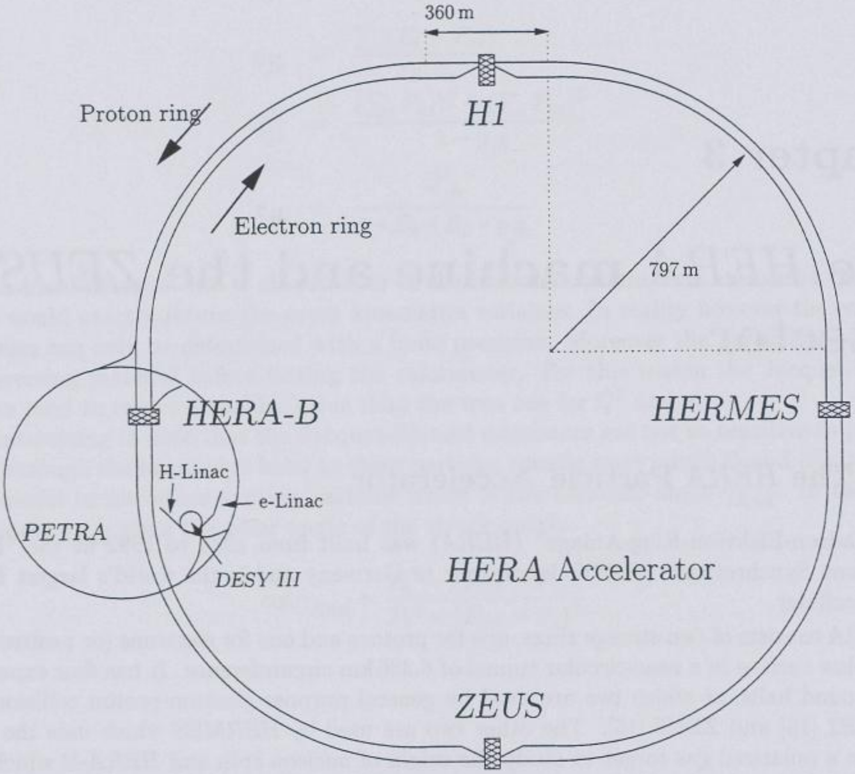

Figure 3.1: Schematic view of the *HERA* collider and its pre-accelerators, the linear accelerators for electrons (or positrons) and protons, the *DESY III* accelerator ring and *PETRA*. The locations of the experiments are also indicated.

3.2 The *ZEUS* Detector

The *ZEUS* detector is a multi purpose *e-p* collision detector. Like other high energy collider experiments the *ZEUS* detector consists of layers of sub-detectors which surround the interaction point. Since the positron and proton beam momentum are so different the detector is asymmetric with respect to the beam direction. Figure 3.2 shows cross sectional views of the *ZEUS* detector. The innermost detector is the vertex detector (*VXD*), followed by the central tracking detector (*CTD*). In the forward direction the tracking is complemented by a forward drift chamber (*FTD*) and transition radiation detector (*TRD*) and in the rear direction a planar drift chamber (*RTD*) is installed. The tracking detectors are surrounded by a super conducting solenoid (*COIL*) which produces a magnetic field of 1.432 Tesla. The next layer consists of the Uranium scintillator calorimeter (*UCAL*). The flux return yoke (*YOKE*) for the solenoidal field is instrumented as backing calorimeter (*BAC*) capable of detecting leakage of particles from the *UCAL*. The inside and outside of the return yoke are instrumented with muon chambers (*FMUON*, *BMUON* and *RMUON*), the forward muon chamber (*FMUON*) is complemented by a toroidal magnet. In the

HERA beams	Electron	Proton
Center of mass energy	314 GeV	
Nominal energy	30 GeV	820 GeV
Relative energy spread $\Delta E/E$	10^{-3}	10^{-4}
Injection energy	12 GeV	40 GeV
Luminosity per interaction point	$1.6 \times 10^{31}\,\mathrm{cm}^{-2}\mathrm{s}^{-1}$	
Average current	58 mA	163 mA
Particles per bunch	3.65×10^{10}	10^{11}
Number of bunches	220	220
Maximum number of filled bunches	210	210
Beam crossing angle	head-on collision, 0 mrad	
Bunch crossing interval	$96\,\mathrm{ns} \simeq 28.8\,m$	
Bunch length at maximum energy (σ_z)	0.85 cm	19 cm
Beam width at the interaction points (σ_x)	0.286 mm	0.28 mm
Beam height at the interaction points (σ_y)	0.06 mm	0.058 mm
Synchrotron radiation loss per turn	125 MeV	6×10^{-10} MeV
Polarization time at 30 GeV	35 min	-
Filling time	15 min	20 min

Table 3.1: Main design parameters of the *HERA* machine.

rear of the *ZEUS* detector the *Vetowall* detector is installed. Close to the beam collimator *C5*, *ZEUS* has a detector (*C5*) which is used to monitor the beam quality and timing. Further away from the interaction point and not shown in figure 3.2 is the luminosity monitor (*LUMI*).

A detailed and complete description of the *ZEUS* detector can be found in [17]. We will concentrate further only on the sub-detectors that were used for the charged current event selection and analysis: *CTD*, *UCAL*, *BMUON*, *RMUON*, *FMUON*, *Vetowall*, *C5* and the luminosity monitor *LUMI*.

3.2.1 Central Tracking Detector (*CTD*)

The Central Tracking Detector (*CTD*) is a cylindrical drift chamber with nine super layers of eight sense wire layers each. Five of the super layers (odd numbered) have wires parallel to the chamber axis, four layers (even numbered) have stereo layers with wires tilted under a small angle (5 ° or 7 °) with respect to the beam. The single wire hit resolution of the *CTD* is $170\,\mu$ m. The chamber covers an angular range of $15° < \theta < 164°$. The *CTD* is read out by two independent readout systems, the "Z-by-timing" and the *FADC* system. The "Z-by-timing" system is used for the layers with the parallel wires and uses the difference between the arrival times of the pulses at the two ends of a wire to determine the Z coordinate. Its Z resolution is about 4 cm. Using the *FADC* system, the combination of the axial and stereo wire information allows the reconstruction of the Z vertex of a track with a precision of 1 mm.

3.2.2 Uranium Scintillator Calorimeter (*UCAL*)

The *ZEUS* high resolution calorimeter is constructed of layers of depleted Uranium and Scintillator. It consists of three sections, forward (*FCAL*), barrel (*BCAL*) and rear (*RCAL*). The forward (*FCAL*) and rear (*RCAL*) calorimeter consist of two halves which can be retracted in order to avoid radiation damage due to beam losses during beam injection.

The *FCAL* and *RCAL* are subdivided in modules of 20 cm width and varying height arranged as shown in figures 3.3 and 3.4. The tallest module has an active height of 4.6 m. Each module consists of towers with a frontal area of $20 \times 20\,\mathrm{cm}^2$. Each tower is segmented in depth in an electromagnetic section (*EMC*) of $25\,\mathrm{X}_0$ and one (*RCAL*) or two (*FCAL*) hadronic (*HAC*) sections. The total depth of the *FCAL* is $7\,\lambda$ and that of the *RCAL* is $5\,\lambda$. The *EMC* sections of the *FCAL* and *RCAL* are further divided vertically in cells of $5 \times 20\,\mathrm{cm}^2$ and $10 \times 20\,\mathrm{cm}^2$ frontal area respectively. A layer of $3 \times 3\,\mathrm{cm}^2$ silicon diodes (*HES*) is placed inside the *EMC* sections at a depth of $3\,\mathrm{X}_0$ to aid in the separation of hadronic and electromagnetic showers.

The *BCAL* consists of 32 "pie shaped" modules arranged concentrically around the beam at a distance of 1.32 m (see figure 3.2). Each module has a length of 3.2 m and subtends 11.25 ° in azimuth. The modules are tilted by 2.5 ° to avoid projective cracks between modules. Each module is subdivided in 14 non projective *HAC* towers, each of which are segmented in two sections in depth. The *HAC* towers are preceded by an *EMC* section divided in 53 cells which have a projective geometry. The perpendicular depth of the *EMC* is $23\,\mathrm{X}_0$ and the total perpendicular depth of the *BCAL* is $5\,\lambda$.

The entire *UCAL* thus consists of 5918 cells. The scintillation light of each cell is guided to the back of the calorimeter via two wavelength shifter (*WLS*) guides, one on either side of each cell. Each *WLS* is read out by a photomultiplier (*PMT*). To reduce the effects of the cracks between modules, in particular the generation of Cherenkov light in the *WLS*, sheets of 4 mm of lead are placed between all the modules.

The energy resolution of the *UCAL* is $\sigma(E)/E = 0.18/\sqrt{E}$ for electromagnetic showers and $\sigma(E)/E = 0.35/\sqrt{E}$ for hadronic showers where the shower energy E is in GeV.

The timing resolution of each individual channel is given by

$$\sigma(T) = 0.4 + 1.4/(E_{ch}^{0.65})(ns) \tag{3.1}$$

where $E_{ch}[GeV]$ is the energy recorded in the channel (see [18]).

The radioactivity of the depleted Uranium causes a constant current drawn by the *PMT*s. The current is proportional to the cell size and used to calibrate the absolute energy scale of the calorimeter [19].

The *UCAL* readout system consists of two systems, one for the *FLT* and one for the *SLT* and higher level triggers. The signal for the *FLT* is split off on the detector and analogue sums of several cells are made. The *SLT* readout system has the higher precision of the full digitized readout.

3.2.3 Forward Muon Chamber

The forward muon chamber (*FMUON*) consists of a toroidal magnetized iron region, interleaved with sections of drift chambers, limited streamer tubes and time of flight counters. The outer diameter of the toroids is 6 m, the magnetic field 1.7 Tesla. The forward muon chambers provide a momentum measurement of muons of energies up to 100 GeV down to low angles.

Barrel and Rear Muon Chamber

In the barrel (*BMUON*) and rear (*RMUON*) muon systems the magnetic field of the iron *YOKE* is used to perform a momentum measurement. Each chamber consists of two layers of limited streamer tubes with wires and perpendicular readout strips mounted on the inside and outside of the iron *YOKE*. For the barrel detector, the wires are in the beam direction, for the rear detector in the Y direction. The hit position resolution is better than 1 mm. The barrel and rear muon detector can be used to measure the momentum of prompt muons but also cosmic muons.

3.2.4 *Vetowall* and *C5* Detector

The *Vetowall* detector is an iron wall of 0.9 m thickness, placed in the upstream proton beam direction closing the accelerator tunnel. It has scintillator counters on both sides of the wall. The *C5* detector consists of 0.5 cm of lead, sandwiched between scintillators, placed around the *C5* beam collimator, at $z = -3.15\,\mathrm{m}$.

3.2.5 Luminosity Detector

In order to do a cross section measurement at a collider experiment the luminosity has to be determined. In order to do so the rate of a process with a well known cross section is measured. This process also has to have a high cross section to be used online so that the beam optics can be modified for maximum luminosity. At *HERA* the hard photon bremsstrahlung produced in the Bethe-Heitler process $ep \to ep\gamma$ [20] is used.

The *ZEUS* luminosity monitor (*LUMI*) consists of two calorimeters, one, for detecting the scattered photon is placed near the proton beam pipe at $Z = -107\,\mathrm{m}$, the other one, for detecting the scattered positron is placed at $Z = -34.7\,\mathrm{m}$. The acceptance for photon detection is 99 % for $E_\gamma > 5\,\mathrm{GeV}$. The positron acceptance is more difficult to estimate because the positrons have to traverse several magnets before reaching the calorimeter, but it is about 70 % for $10\,\mathrm{GeV} < E_e < 17\,\mathrm{GeV}$. The coincidence rate of the two calorimeters is used as a cross check for the luminosity determined from the photon counter only.

The luminosity detector of *ZEUS* and its operation are described in detail in [21, 22].

The data used for this thesis is the positron-proton data of 1994, for which *HERA* delivered a luminosity of $5.11\,\mathrm{pb}^{-1}$. Of this luminosity, *ZEUS* could trigger $3.3\,\mathrm{pb}^{-1}$, the difference being mainly due to the time necessary for the beam conditions to stabilize at the beginning of each run. Some losses were due to miscellaneous detector problems.

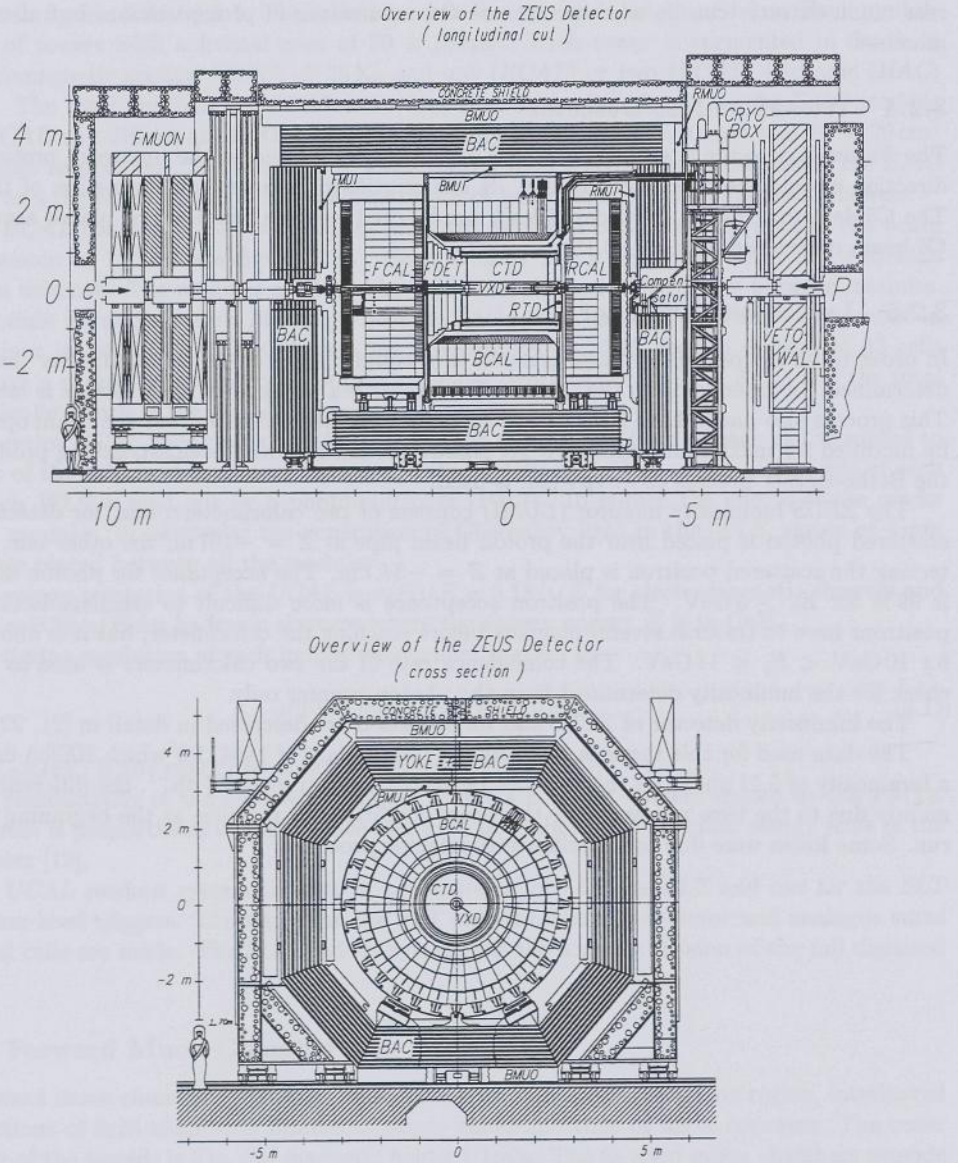

Figure 3.2: Cross section of the *ZEUS* detector along the beam line (top picture) and perpendicular to it (bottom picture).

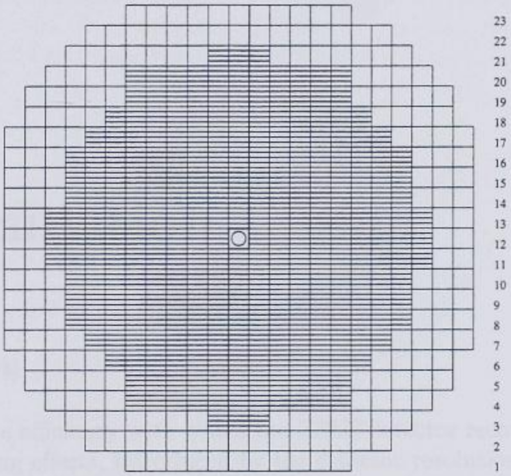

Figure 3.3: Schematic view of the front face of the *FCAL*.

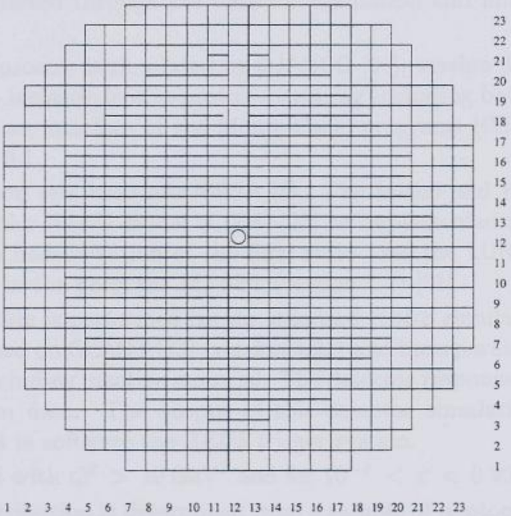

Figure 3.4: Schematic view of the front face of the *RCAL*.